Behavioral/Cognitive

Social Play Behavior Is Critical for the Development of Prefrontal Inhibitory Synapses and Cognitive Flexibility in Rats

Ate Bijlsma,[1,2*] Azar Omrani,[1,3*] Marcia Spoelder,[2*] Jeroen P.H. Verharen,[2,3] Lisa Bauer,[1] Cosette Cornelis,[2] Beleke de Zwart,[2] René van Dorland,[1] Louk J.M.J. Vanderschuren,[2] and Corette J. Wierenga[1]

[1]Department of Biology, Faculty of Science, Utrecht University, 3584 CH, Utrecht, The Netherlands, [2]Department of Population Health Sciences, Section Animals in Science and Society, Faculty of Veterinary Medicine, Utrecht University, 3584 CM, Utrecht, The Netherlands, and [3]Department of Translational Neuroscience, University Medical Center Utrecht, 3584 CG, Utrecht, The Netherlands

Sensory driven activity during early life is critical for setting up the proper connectivity of the sensory cortices. We ask here whether social play behavior, a particular form of social interaction that is highly abundant during postweaning development, is equally important for setting up connections in the developing prefrontal cortex (PFC). Young male rats were deprived from social play with peers during the period in life when social play behavior normally peaks [postnatal day 21–42] (SPD rats), followed by resocialization until adulthood. We recorded synaptic currents in layer 5 cells in slices from medial PFC of adult SPD and control rats and observed that inhibitory synaptic currents were reduced in SPD slices, while excitatory synaptic currents were unaffected. This was associated with a decrease in perisomatic inhibitory synapses from parvalbumin-positive GABAergic cells. In parallel experiments, adult SPD rats achieved more reversals in a probabilistic reversal learning (PRL) task, which depends on the integrity of the PFC, by using a more simplified cognitive strategy than controls. Interestingly, we observed that one daily hour of play during SPD partially rescued the behavioral performance in the PRL, but did not prevent the decrease in PFC inhibitory synaptic inputs. Our data demonstrate the importance of unrestricted social play for the development of inhibitory synapses in the PFC and cognitive skills in adulthood and show that specific synaptic alterations in the PFC can result in a complex behavioral outcome.

Key words: **brain development; cognitive performance; experience-dependent plasticity; prefrontal cortex; social play; synaptic currents**

Significance Statement

This study addressed the question whether social play behavior in juvenile rats contributes to functional development of the prefrontal cortex (PFC). We found that rats that had been deprived from juvenile social play (social play deprivation - SPD) showed a reduction in inhibitory synapses in the PFC and a simplified strategy to solve a complex behavioral task in adulthood. Providing one daily hour of play during SPD partially rescued the cognitive skills in these rats, but did not prevent the reduction in PFC inhibitory synapses. Our results demonstrate a key role for unrestricted juvenile social play in PFC development and emphasize the complex relation between PFC circuit connectivity and cognitive function.

Received Mar. 11, 2022; revised Aug. 12, 2022; accepted Sep. 20, 2022.

Author contributions: A.B., A.O., L.J.M.J.V., and C.J.W. designed research; A.B., A.O., M.S., L.B., C.C., and B.d.Z. performed research; A.B., A.O., M.S., J.P.H.V., L.B., C.C., B.d.Z., and R.v.D. analyzed data; A.B. wrote the first draft of the paper; A.B., L.J.M.J.V., and C.J.W. edited the paper; L.J.M.J.V. and C.J.W. wrote the paper.

This work was supported by the Netherlands Organization for Scientific Research (NWO) Grant ALWOP.2015.105 (to L.J.M.J.V. and C.J.W.) and Utrecht University strategic theme Dynamics of Youth. We thank Daniëlle Counotte for preliminary experiments and Ruth Damsteegt for practical assistance.

A. Omrani's present address: Department of CNS Diseases Research, Boehringer Ingelheim Pharma GmbH & Co KG, Biberach, Germany.

M. Spoelder's present address: Department of Cognitive Neuroscience, Donders Institute for Brain, Cognition and Behavior, Radboud University Nijmegen Medical Center, Nijmegen, The Netherlands.

J.P.H. Verharen's present address: Helen Wills Neuroscience Institute, Department of Molecular and Cell Biology, University of California Berkeley, Berkeley, California.

*A.B., A.O., and M.S. contributed equally to this work.

The authors declare no competing financial interests.

Correspondence should be addressed to Corette J. Wierenga at c.j.wierenga@uu.nl or Louk J.M.J. Vanderschuren at l.j.m.j.vanderschuren@uu.nl.

https://doi.org/10.1523/JNEUROSCI.0524-22.2022

Introduction

The developing brain requires proper external input to fine-tune activity and connectivity in neural circuits to ensure optimal functionality throughout life. This process has been extensively studied in the sensory cortices, and it is long known that sensory deprivation during development causes long-lasting deficits in sensory processing resulting from improper synaptic wiring (Hensch, 2005; Gainey and Feldman, 2017). However, how experience-dependent plasticity contributes to the development of other brain structures, such as the prefrontal cortex (PFC), remains largely unknown (Kolb et al., 2012; Larsen and Luna, 2018; Reh et al., 2020).

The PFC is important for higher cognitive, so-called executive functions (Miller and Cohen, 2001; Floresco et al., 2008), as well as neural operations required during social interactions (Frith and Frith, 2012; Rilling and Sanfey, 2011). By analogy of sensory cortex development, proper PFC development may require complex cognitive and social stimuli. Importantly, during the period when the PFC matures, i.e., in between weaning and early adulthood (Kolb et al., 2012), young animals display an abundance of an energetic form of social behavior known as social play behavior (Panksepp et al., 1984; Vanderschuren et al., 1997; Pellis and Pellis, 2009). Social play behavior involves PFC activity (van Kerkhof et al., 2013b), and lesions or inactivation of the PFC have been found to impair social play (Bell et al., 2009; van Kerkhof et al., 2013a). It is widely held that exploration and experimentation during social play facilitates the development of a rich behavioral repertoire, that allows an individual to quickly adapt in a changeable world. In this way, social play subserves the development of PFC-dependent skills such as flexibility, creativity, and decision-making (Spinka et al., 2001; Pellis and Pellis, 2009; Vanderschuren and Trezza, 2014).

The developmental changes in the PFC circuitry that facilitate these cognitive skills are incompletely understood. Lack of social play experience during postweaning development has been reported to cause long-lasting changes in PFC circuitry and function (Leussis et al., 2008; Bell et al., 2010; Baarendse et al., 2013; Vanderschuren and Trezza, 2014). However, the cellular mechanisms by which social play facilitates PFC development remain elusive. It is well described that sensory deprivation induces specific alterations in inhibitory neurotransmission that affect adult sensory processing (Turrigiano and Nelson, 2004; Hensch, 2005; Rupert and Shea, 2022). We therefore hypothesized that early life social experiences specifically shape PFC inhibition. To test this, we here investigated how cognitive flexibility and inhibitory signaling in the adult PFC are affected when rats are deprived from social play behavior during development.

Materials and Methods

Animals and housing conditions

All experimental procedures were approved by the Animal Ethics Committee of Utrecht University and the Dutch Central Animal Testing Committee and were conducted in accordance with Dutch (Wet op de Dierproeven, 1996; Herziene Wet op de Dierproeven, 2014) and European legislation (Guideline 86/609/EEC; Directive 2010/63/EU). Male Lister Hooded rats were obtained from Charles River on postnatal day (P)14 in litters with nursing mothers. The rats were housed under a reversed 12/12 h light/dark cycle with *ad libitum* access to water and food. Rats were weaned on P21 and allocated to either one of the social play deprivation (SPD and SPD1h) groups or the control (CTL) group. Control (CTL) rats were housed with a littermate during the entire experiment. SPD and SPD1h rats were also housed in pairs with a littermate, but between P21 and P42, a transparent Plexiglas divider containing small holes was placed in the middle of the home cage, creating two separate but identical compartments. These holes made it possible for the rats to see, smell and hear each other and to have limited physical interaction without the opportunity to play. SPD1h animals were housed similarly to the SPD group but were allowed to socially interact with their cage mate for 1 h/d. Social interaction sessions took place in a Plexiglas arena of 40 × 40 × 60 cm (l × w × h) with ~2 cm of wood shavings. The social interaction sessions were recorded and the behavior was manually scored per pair using the Observer XT 15 software (Noldus Information Technology BV). Four behaviors were scored:

- Frequency of pinning: one animal lying with its dorsal surface on the floor with the other animal standing over it.
- Frequency of pouncing: one animal attempts to nose/rub the nape of the neck of the partner.
- Time spent in social exploration: one animal sniffing or grooming any part of the partner's body.
- Time spent in nonsocial exploration: the animals exploring the cage or walk around.

Of these behaviors, pinning and pouncing are considered the most characteristic parameters of social play behavior in rats (Panksepp and Beatty, 1980; Vanderschuren et al., 1995b).

A total of 10 pairs was recorded during their social interaction sessions. Four of these were eventually used for the electrophysiology experiments while the other six pairs were used for behavioral testing.

On P42, the Plexiglas divider was removed and SPD and SPD1h rats were housed in pairs for the remainder of the experiment. SPD animals, but not SPD1h rats, showed enhanced and somewhat altered play on resocialization. However, this behavior normalized within a week and after that, all animals behaved indistinguishably from each other. All rats were housed in pairs for at least four weeks until early adulthood (10 weeks of age) after which experimentation began. All experiments were conducted during the active phase of the animals (10 A.M. to 5 P.M.). One week before the start of testing, the rats were subjected to food-restriction and were maintained at 85% of their free-feeding weight for the duration of the behavioral experiment. Rats were provided with ~20 sucrose pellets (45 mg, BioServ) in their home cage for two subsequent days before their first exposure to the operant conditioning chamber to prevent potential food neophobia. Rats were weighed and handled at least once a week throughout the course of the experiment.

Probabilistic reversal learning (PRL)

Apparatus

Behavioral testing was conducted in operant conditioning chambers (Med Associates) enclosed in sound-attenuating cubicles equipped with a ventilation fan. Two retractable levers were located on either side of a central food magazine into which sugar pellets could be delivered via a dispenser. A LED cue light was located above each retractable lever. A white house light was mounted in the top-center of the wall opposite the levers. Online control of the apparatus and data collection was performed using MED-PC (Med Associates) software.

Pretraining

Rats were habituated once to the operant chamber for 30 min in which the house light was illuminated and 50 sucrose rewards were randomly delivered into the magazine with an average of 15 s between reward deliveries. On the subsequent days, the rats were trained for 30 min under a fixed-ratio 1 (FR1) schedule of reinforcement for a minimum of three consecutive sessions. The session started with the illumination of the house light and the insertion of both levers, which remained inserted for the remainder of the session. One of the two levers was the "correct" lever rendering a reward when pressed, whereas pressing the other lever had no consequences. There was no limit other than time on the amount of times a rat could press the "correct" lever. If the rat obtained 50 or more rewards in a session it was required to press the other lever the following day. If it obtained <50 rewards the rat was tested on the same

Table 1. Overview of computational models

Model family	#	Model name	n_f	Description
Random choice	1	Random choice model	0	Animal choses randomly.
Heuristics family	2	Win-Stay, Lose-Switch	1	Animal stays on the same lever after winning, moves away from the lever after a loss.
	3	Win-Stay, Lose-Random	1	Animal stays on the same lever after winning, randomly picks a lever after a loss.
	4	Random choice + stickiness	2	Animal choses randomly but attributes value to the lastly chosen lever (Verharen et al., 2020).
Q learning family	5	Q learning, single learning rate for reward and punishment learning	2	Animal learns from previous decisions. Learning rate for positive and negative feedback are the same (Verharen et al., 2020).
	6	Q learning, separate learning rates for reward and punishment learning	3	Animal learns from previous decisions. Learning rate for positive and negative feedback may differ (Verharen et al., 2020).
	7	Model 6 + stickiness parameter	4	Animal learns from previous decisions. Learning rate for positive and negative feedback are separately calculated. Additionally, the animal attributes value to the lastly chosen lever (Verharen et al., 2020).
	8	Rescorla–Wagner Pearce–Hall	4	Animal learns from previous decisions. Learning rate for positive and negative feedback are the same. Additionally, the animal may learn better when task volatility is higher (e.g., after a reversal).

schedule the next day. Next, the animals were familiarized with lever insertion and retraction, in daily sessions that lasted 100 trials or 60 min, whichever occurred first. A trial started with an intertrial interval (ITI) of 5 s with the chamber in darkness, followed by the illumination of the house-light and the insertion of one of the two levers into the chamber. A response within 30 s on the inserted lever resulted in the delivery of a reward. If the rat failed to respond on the lever within 30 s, the lever retracted and the trial was scored as an omission. Rats were trained for ~3–4 d to a criterion of at least 50 rewards and had to perform a lever press in >80% of the trials before progressing to the probabilistic reversal learning.

Probabilistic reversal learning

The protocol used for this task was modified from those of previous studies (Bari et al., 2010; Dalton et al., 2016; Verharen et al., 2020). At the start of each session one of the two levers was randomly selected to be "correct" and the other "incorrect." A response on the "correct" lever resulted in the delivery of a reward on 80% of the trials, whereas a response on the "incorrect" lever was reinforced on 20% of trials. Each trial started with a 5-s ITI, followed by the illumination of the house-light and the insertion of both levers into the chamber. After a response, both levers retracted. In case the rat was rewarded, the house light remained illuminated, whereas the house light extinguished in case the rat was not rewarded on the "correct" lever. An "incorrect" response or a failure to respond within 30 s after lever insertion (i.e., omission) lead to the retraction of both levers, extinction of the house light so that the chamber returned to its ITI state. When the rat made a string of eight consecutive trials on the "correct" lever (regardless of whether they were rewarded or not), contingencies were reversed, so that the "correct" lever became the "incorrect" lever and the previously "incorrect" lever became the "correct" lever. This pattern repeated over the course of a daily session. Daily sessions lasted for 200 trials or after 60 min had passed, whichever occurred first. The average session time was 29 ± 3 min (range 24–50 min) and there were no differences between groups ($p = 0.43$ and $p = 0.85$ for batch 1 and batch 2, respectively; batch 1 vs batch 2: $p = 0.16$).

Trial-by-trial analysis

This analysis was performed to assess the shifts in choice behavior between subsequent trials, to investigate the sensitivity to positive and negative feedback. Depending on whether the rat received a reward or not, it can press the same lever on the subsequent trial or shift toward the other lever, resulting in 4 different choices (i.e., win-stay, win-shift, lose-stay, lose-shift) for both the "correct" and "incorrect" lever. We calculated these choices (win-stay vs win-shift and lose-stay vs lose-shift) as percentages per session.

Normalization

The PRL task was performed twice with two different batches of animals. The first batch consisted of 12 CTL and 12 SPD animals. The second batch consisted of three groups of 12 rats (CTL, SPD, and SPD1h). Rats in the second batch overall made a higher number of reversals performed generally better than in the first batch (CTL rats made 2.8 ± 0.6 reversals in batch 1 and 5.0 ± 1.3 in batch 2; $p < 0.0001$). We verified that our conclusions were supported by each batch separately. To compare the number of reversals between the groups in both batches we used the following normalization using the minimum (*groupmin*) and maximum (*groupmax*) values per group: $x' = \frac{x - groupmin}{groupmax - groupmin}$, in which x is the original individual value and x' is the normalized value. To compare the win-stay and lose-shift choices per session for the pooled data, we normalized the SPD and SPD1h data to the average of their respective control group.

Computational modelling

Eight different computational models were fit to the trial-by-trial responses to assess differences in task strategy between the three groups of animals. Best-fit model parameters were estimated using maximum likelihood estimation, using MATLAB (version 2018b; The MathWorks Inc.) function *fmincon* (Verharen et al., 2018). These maximum likelihood estimates were corrected for model complexity [i.e., the number of free parameters (n_f)] by calculating the Akaike information criterion (AIC) for each session:

$$\mathrm{AIC} = 2 * n_f - 2 * log(likelihood),$$

in which a lower AIC indicates more evidence in favor of the model. These log-model evidence estimates were subsequently used to perform Bayesian model selection (Rigoux et al., 2014) using the MATLAB package SPM12 (The Wellcome Center for Human Neuroimaging), taking into account the family to which each model belonged (Penny et al., 2010). This yielded the protected exceedance probability for the 8 individual models and for each family of models (random choice, heuristic and Q learning family), indicating the probability that each of the (family of) models was most prevalent in the group of rats.

Table 1 contains an overview of the eight computational models. The random choice model is the null model, which assumes that animals choose randomly [i.e., $p = 0.5$ for each choice, so that the log likelihood is given by [number of trials]*log(0.5)]. The second family of models contained strategies based on "heuristics"; simple strategies to complete the task. The third family contained Q learning models, consisting of four derivatives of the Rescorla–Wagner model (Rescorla and Wagner, 1972).

In all models (except for the random choice model), choice was modeled using a Softmax equation, such that the probability of choosing the left lever in trial t was given by:

$$p_{left,t} = \frac{\exp(\beta \cdot Q_{left,t})}{\exp(\beta \cdot Q_{left,t}) + \exp(\beta \cdot Q_{right,t})},$$

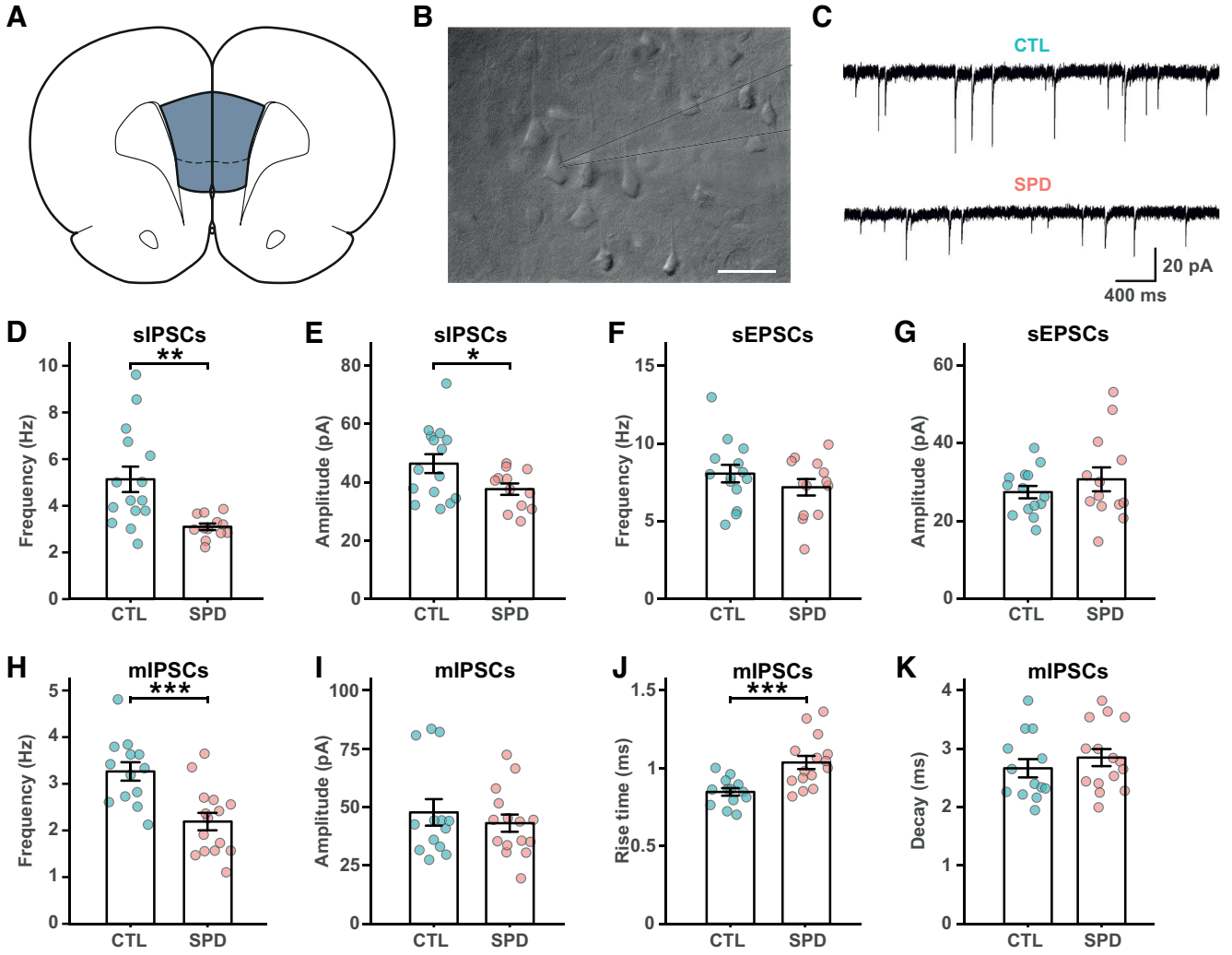

Figure 1. Reduced prefrontal inhibition in L5 pyramidal cells after social play deprivation. ***A***, Schematic diagram depicting the recording site in the mFPC. ***B***, Microscope image of L5 cells in the mPFC with the recording electrode (gray lines). Scale bar is 20 μm. ***C***, Example traces of spontaneous IPSCs (sIPSCs) in L5 pyramidal cells in slices from control (CTL) and social play deprived (SPD) rats. ***D***, ***E***, Frequency (***D***) and amplitude (***E***) of sIPSCs in CTL and SPD slices ($p = 0.002$ and $p = 0.03$; *t* test). ***F***, ***G***, Frequency (***F***) and amplitude (***G***) of spontaneous EPSCS (sEPSCs) ($p = 0.27$ and $p = 0.35$; *t* test). ***H***, ***I***, Frequency (***H***) and amplitude (***I***) of miniature IPSCS (mIPSCs) ($p < 0.0005$ and $p = 0.50$; *t* test). ***J***, Rise time of mIPSCs ($p = 0.0008$; *t* test). ***K***, Decay time of mIPSCs ($p = 0.40$; *t* test). Data from 15 CTL and 13 SPD brain slices (6 rats per group). Statistical range: $^*p \leq 0.05$, $^{**}p < 0.01$, $^{***}p < 0.001$.

in which β is the Softmax' inverse temperature (which was a free parameter in models 2 through 8), and Q is the value of the lever.

For models that included a stickiness parameter, the Softmax was given by:

$$p_{left,t} = \frac{\exp(\beta \cdot Q_{left,t} + \pi \cdot \varphi_{left,t-1})}{\exp(\beta \cdot Q_{left,t} + \pi \cdot \varphi_{left,t-1}) + \exp(\beta \cdot Q_{right,t} + \pi \cdot \varphi_{right,t-1})}.$$

In this equation, π is the stickiness parameter, φ is a Boolean that was 1 when that lever was chosen in the previous trials, and 0 otherwise.

After each trial outcome, lever values Q_{left} and Q_{right} were updated according to a Q learning rule:

$$Q_{left,t} = Q_{left,t} + \alpha \cdot RPE_t.$$

Here, α is the learning rate, and RPE_t indicates the reward prediction error on trial *t*. In turn, the reward prediction error was given by:

$$RPE_t = \begin{cases} 1 - Q_{s,t-1} \text{ for win trials} \\ 0 - Q_{s,t-1} \text{ for lose trials} \end{cases},$$

in which $Q_{s,t-1}$ represents the expected reward value of the chosen lever Q_s.

Electrophysiological analysis

The electrophysiological experiments were conducted in two batches, which were performed by different researchers using different recording protocols with several years in between. The first batch consisted of 12 CTL and 12 SPD animals. The second batch consisted of three groups of 12 rats (CTL, SPD, and SPD1h). For slice preparation, rats (12–15 weeks of age) were anesthetized by intraperitoneal injection of sodium pentobarbital (batch 1) or induction with isoflurane (batch 2) and then transcardially perfused with ice-cold modified artificial CSF (ACSF) containing (in mM): 92 *N*-methyl-D-glutamine (NMDG), 2.5 KCl, 1.25 NaH_2PO_4, 30 $NaHCO_3$, 20 HEPES, 25 glucose, 2 thiourea, 5 Na-ascorbate, 3 Na-pyruvate, 0.5 $CaCl_2.4H_2O$, and 10 $MgSO_4.7H_2O$, bubbled with 95% O_2 and 5% CO_2 (pH 7.3–7.4). For batch 2, NMDG was replaced by choline chloride and thiourea was left out. Coronal slices of the medial PFC (mPFC; 300 µm) were prepared using a vibratome (Leica VT1200S, Leica Microsystems) in ice-cold modified ACSF. Slices were initially incubated in the carbogenated modified ACSF for 5–10 min at 34° C and then transferred into a holding chamber containing standard ACSF containing (in mM): 126 NaCl, 3 KCl, 2 $MgSO_4$, 2 $CaCl_2$, 10 glucose, 1.25 NaH_2PO_4, and 26 $NaHCO_3$ bubbled with 95% O_2 and 5% CO_2 (pH 7.3) at room temperature (RT) for at least 30 min (2 $MgSO_4$ was replaced by 1.3 $MgCl_2$ in batch 2). They were subsequently transferred to the recording chamber, perfused with

standard ACSF that is continuously bubbled with 95% O_2 and 5% CO_2 at 28–32°C.

Whole-cell recordings and analysis

Whole-cell patch-clamp recordings were performed from layer 5 (L5) pyramidal neurons in the medial PFC. We chose to study L5 cells, because these are the main output neurons of the PFC (Douglas and Martin, 2004). These neurons were visualized with an Olympus BX61W1 microscope using infrared video microscopy and differential interference contrast (DIC) optics. Patch electrodes were pulled from borosilicate glass capillaries and had a resistance of 3–6 MΩ when filled with intracellular solutions. EPSCs were recorded in the presence of bicuculline (10 μM) and with internal solution containing (in mM): 140 K-gluconate, 1 KCl, 10 HEPES, 0.5 EGTA, 4 MgATP, 0.4 Na_2GTP, 4 Na_2phosphocreatine (pH 7.3 with KOH). IPSCs were recorded in the presence of 6-cyano-7-nitroquinoxaline-2,3-dione (CNQX; 10 μM in batch 1; 20 μM in batch 2) and D,L-2-amino-5-phosphopentanoic acid (D,L-AP5; 20 μM in batch 1; 50 μM in batch 2), with internal solution containing (in mM): 125 CsCl, 2 $MgCl_2$, 5 NaCl, 10 HEPES, 0.2 EGTA, 4 MgATP, 0.4 Na_2GTP (pH 7.3 with CsOH; batch 1) or 70 K-gluconate, 70 KCl, 10 HEPES, 0.5 EGTA, 4 MgATP, 0.4 Na_2GTP, 4 Na_2phosphocreatine (pH 7.3 with KOH; batch 2). Action-potential independent miniature IPSCs (mIPSCs) were recorded under the same conditions, but in the presence of 1 μM tetrodotoxin (TTX; Sigma) to block sodium channels. The membrane potential was held at −70 mV for voltage-clamp experiments. Signals were amplified, filtered at 3 kHz and digitized at 10 kHz using an EPC-10 patch-clamp amplifier with PatchMaster v2x73 software (batch 1) or MultiClamp 700B amplifier (Molecular Devices) with pClamp 10 software (batch 2). Series resistance was constantly monitored, and the cells were rejected from analysis if the series resistance changed by >20% or exceeded 30 MΩ. No series resistance compensation was used. Resting membrane potential was measured in bridge mode (I = 0) immediately after obtaining whole-cell access. The basic electrophysiological properties of the cells were determined from the voltage responses to a series of hyperpolarizing and depolarizing square current pulses. Input resistance was determined by the slope of the linear regression line through the voltage-current curve. Passive and active membrane properties were analyzed with Clampfit 10 (Axon Instrument) or MATLAB (The MathWorks Inc.). Miniature and spontaneous synaptic currents (IPSCs and EPSCs) data were analyzed with Mini Analysis (Synaptosoft Inc.). All events were detected with a criterion of a threshold >3× root-mean-square (RMS) of baseline noise. The detected currents were manually inspected to exclude false events.

Table 2. Primary antibodies for interneuron analysis

Host	Epitope	Concentration	Company	Order number
Rat	Ctip2	1:1000	Abcam	ab18465
Rabbit	PV	1:1000	Life Technologies	PA1933
Mouse IgG1	NeuN	1:500	Millipore	MAB377
Mouse IgG2a	GAD67	1:500	Millipore	MAB5406

Table 3. Secondary antibodies for interneuron analysis

Host	Epitope	Fluorophore	Concentration	Company	Order number
Goat	Anti-rat	Alexa Fluor 568	1:500	Life Technologies	A11077
Goat	Anti-rabbit	Alexa Fluor 405	1:500	Life Technologies	A31556
Goat	Anti-mouse IgG1	Alexa Fluor 647	1:500	Life Technologies	A21240
Goat	Anti-mouse IgG2a	Alexa Fluor 488	1:500	Life Technologies	A21131

Table 4. Primary antibodies for synapse analysis

Host	Epitope	Concentration	Company	Order number
Chicken	VGAT	1:1000	Synaptic Systems	131006
Rabbit	PV	1:1000	Life Technologies	PA1933
Guinea pig	NeuN	1:500	Millipore	ABN90
Mouse	CB1-R	1:1000	Synaptic Systems	258011

Table 5. Secondary antibodies for synapse analysis

Host	Epitope	Fluorophore	Concentration	Company	Order number
Goat	Anti-chicken	Alexa Fluor 647	1:500	Life Technologies	A21449
Goat	Anti-rabbit	Alexa Fluor 405	1:500	Life Technologies	A31556
Goat	Anti-guinea pig	Alexa Fluor 568	1:500	Life Technologies	A11075
Goat	Anti-mouse	Alexa Fluor 488	1:500	Life Technologies	A11029

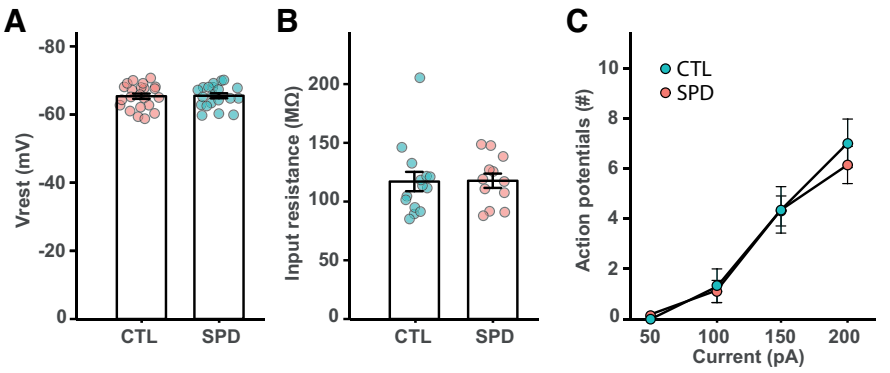

Figure 2. Passive membrane properties of L5 cells are similar in SPD and CTL slices. ***A***, Resting potential of L5 pyramidal neurons in CTL and SPD slices ($p = 0.97$; t test). ***B***, Input resistance ($p = 0.61$; MW test). ***C***, Number of action potentials after current injections in CTL and SPD neurons ($p = 0.58$; two-way ANOVA, condition). Data in ***A*** is from 20 CTL and 22 SPD cells; in ***B*** from 14 CTL and 12 SPD cells; in ***C*** from 19 CTL and 22 SPD cells.

Immunohistochemistry

Tissue preparation

Rats were anesthetized with Nembutal (240 mg/kg, i.p.) and transcardially perfused with 0.1 M PBS (pH 7.3–7.4) followed by 4% paraformaldehyde in 0.01 M PBS. The brains were removed from the skull and postfixed overnight in the same paraformaldehyde solution at 4°C and subsequently cryoprotected in 30% sucrose for 3 d at 4°C. Thereafter, the brains were rapidly frozen in aluminum foil on dry ice and stored at −80°C until further use. Brain sections (20 μm thick) from the PFC between Bregma levels of 4.2–2.2 mm (Paxinos and Watson, 2007) were made with a Cryostat Leica CM 3050 S. Sections were stored at −80°C until immunohistochemistry was performed. Brain slices were thawed and let dry for 1 h at room temperature (RT). Slices were washed in PBS three times for 15 min (3 × 15 min) at RT. Sections were cooked in sodium citric acid buffer (SCAB; 10 mM sodium citric acid in demi water, pH 6) for 10 min at 97°C in a temperature-controlled microwave, cooled for 30 min at 4°C and washed again (3 × 15 min in PBS). Slices were blocked with 400 µl of blocking buffer (10% normal goat-serum, 0,2% Triton X-100 in PBS) for 2 h in a wet chamber at RT. Slices were incubated overnight at 4°C in the wet chamber with 250 µl of primary antibodies in blocking buffer. Sections were washed (3 × 15 min in PBS), followed by incubation with the secondary antibodies in blocking buffer for 2 h at RT in a wet chamber. After another wash step (3 × 15 min in PBS), slides were mounted and stored at 4°C until image acquisition. Primary and secondary antibodies are listed in Tables 2 and 3 (for cell density analysis) and Tables 4 and 5 (for synaptic puncta analysis).

Image acquisition and analysis

Images were taken with a Zeiss Confocal microscope (type LSM700). The investigator was blinded to the groups of the sections when

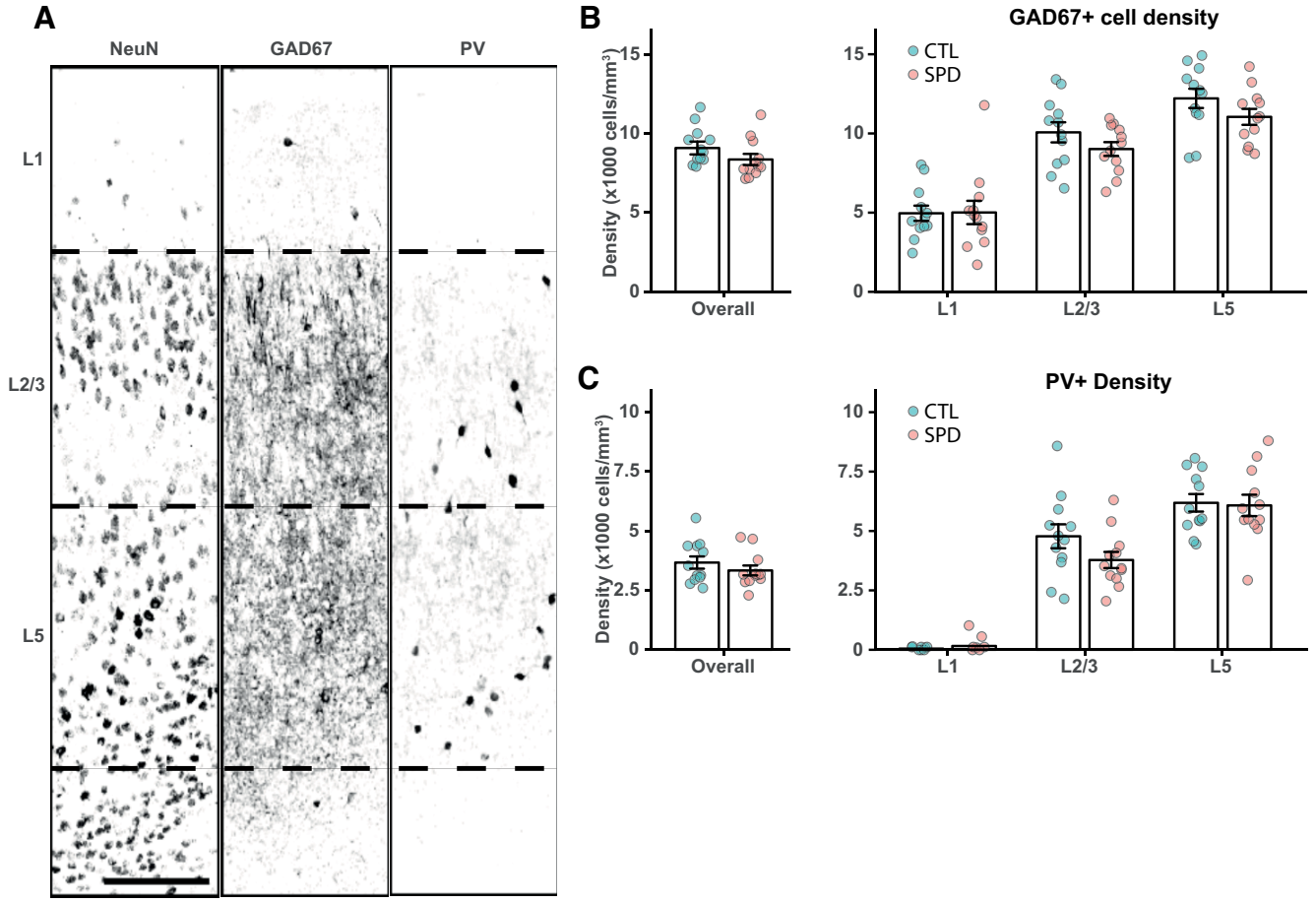

Figure 3. Interneuron density is similar in CTL and SPD tissue. ***A***, Representative confocal image of NeuN, GAD67, and PV-positive neurons in prelimbic cortex layers. Borders between layers are denoted by the dashed lines. Scale bar is 10 μm. ***B***, Left, The average density of GAD67-positive cells in the mPFC over all layers ($p = 0.19$; *t* test). Right, GAD67 cell density in layer 1 ($p = 0.95$; *t* test), layer 2/3 ($p = 0.19$; *t* test), and layer 5 ($p = 0.15$; *t* test). ***C***, Left, The average density of PV-positive cells in the mPFC over all layers ($p = 0.33$; *t* test). Right, PV cell density in layer 1 ($p = 0.90$; MW test), layer 2/3 ($p = 0.12$; *t* test), and layer 5 ($p = 0.85$; *t* test). Data in ***B*** and ***C*** from six CTL and six SPD rats. For each rat, two measurements (from both hemispheres) were included.

acquiring the images and performing the quantifications. Image analysis was performed in ImageJ (National Institutes of Health).

Cell density analysis

z-stacks were acquired at 20× of all layers of the mPFC. Tile scan z-stacks (1600 × 1280 μm^2, 2-μm steps, total of 10 μm) were acquired of the mPFC in both hemispheres of control ($n = 6$) and SPD ($n = 6$) rats. Antibodies staining for NeuN, Ctip2, GAD67, and parvalbumin (PV) were used. NeuN (neuronal nuclei) is a nuclear protein specific for neurons and was used as a marker to identify neurons. Expression of Ctip2 [CtBP (C-terminal binding protein) interacting protein] is restricted to L5/6 and was used to facilitate identification of the cortical layers. The GABA synthesis enzyme GAD67 (glutamate decarboxylase) and the calcium-buffering protein PV were used to identify inhibitory cells.

Synapse analysis

Z-stacks were acquired at 63× in layer 5 of the mPFC. For each of the rat brains [Control ($n = 6$), SPD ($n = 6$)] z-stacks (102 × 102 μm^2, 0.4-μm steps, total of 12 μm) were acquired in both hemispheres. Image analysis was performed semi-automatically using custom-written ImageJ macros and MATLAB scripts. NeuN was used to determine the outline of individual L5 cell somata. VGAT (vesicular GABA transporter) is expressed in all inhibitory synapses and was used as a general inhibitory synaptic marker. For each L5 cell, a maximum intensity image was constructed from 4 z-stack slices, which was median filtered and thresholded. Only synaptic puncta larger than 0.2 μm and with a circularity of 0.6–1.0 that were inside of the 1.5-μm band around the NeuN outline were included. PV and cannabinoid receptor 1 (CB1-R) puncta were only included when co-localized with VGAT.

Data processing and statistical analyses

Statistical analyses were performed with GraphPad Prism (Software Inc.) and RStudio 1_2_5019 (R version 3.6.1, R Foundation for Statistical Computing). Normality of the data was tested with a Shapiro–Wilk test. Differences between two groups were then tested with a nonparametric Mann–Whitney–Wilcoxon (MW) test, or a parametric Welch *t* test (T). Differences between three groups were tested with one-way ANOVA followed up with a Tukey's test. In the electrophysiology and immunocytochemistry datasets the variance between cells or regions of interest (ROIs) within slices was larger than the variance between slices, indicating that individual cells and ROIs can be treated as independent measurements. Behavior in the PRL was analyzed using two-way repeated measures ANOVA (with sessions as within-subjects factor and housing condition as between-subjects factor) followed by *t* tests (with Bonferroni correction). All graphs represent the mean ± SEM with individual data points shown in colored circles.

Results

Rats were deprived of social play for a period of three weeks post-weaning (P21–P42), which is the period in life when social play is most abundant (Baenninger, 1967; Meaney and Stewart, 1981; Panksepp, 1981). Rats in the social play deprivation (SPD) group

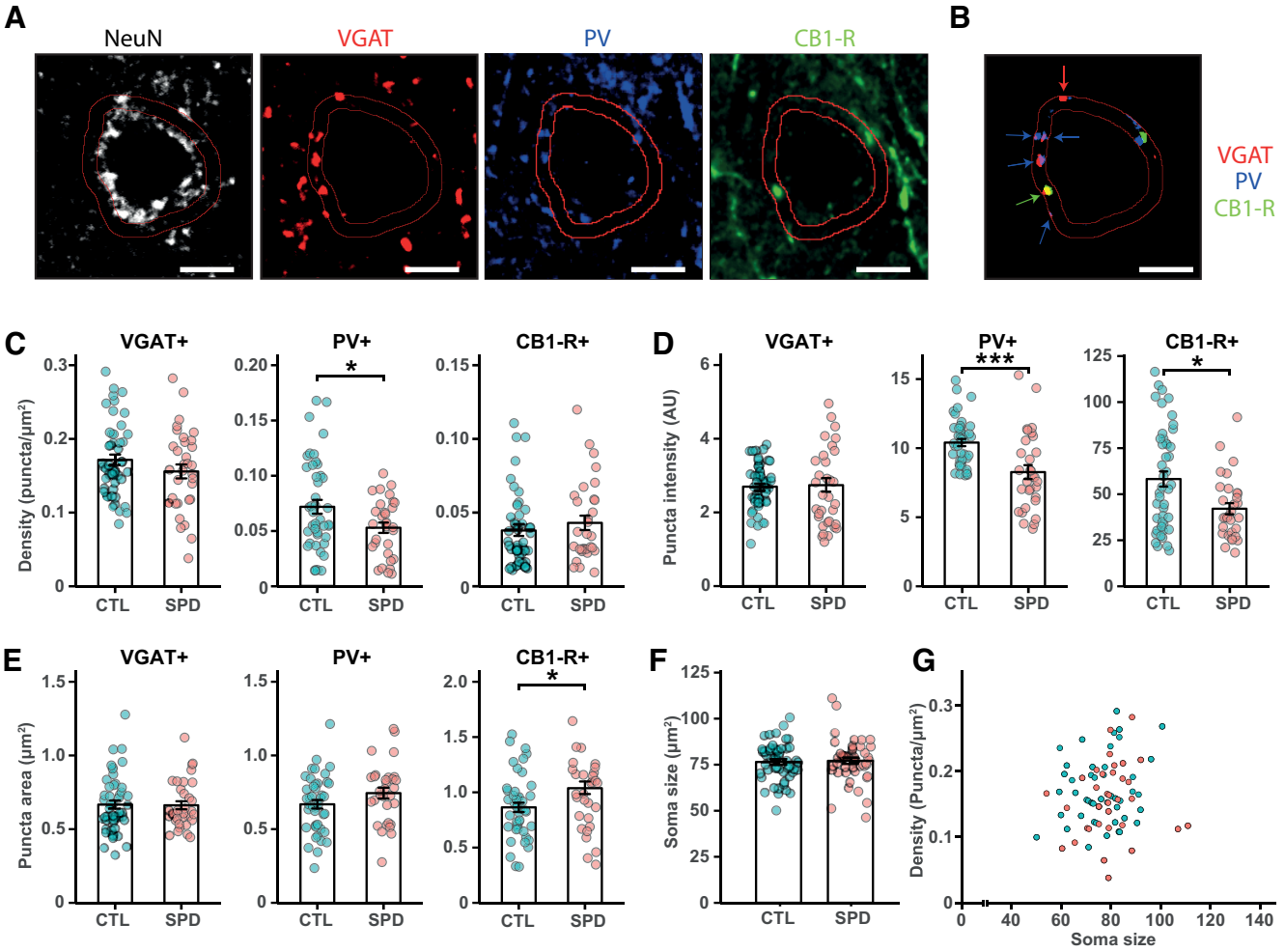

Figure 4. Reduction in perisomatic inhibitory synapses after SPD. ***A***, Representative confocal images for VGAT, PV, CB1-R, and NeuN immunostaining. Scale bar is 1 μm. A 1.5-μm band around the soma was drawn based on the NeuN staining. Individual puncta were selected after thresholding. Only PV and CB1-R puncta that co-localized with VGAT were considered synaptic puncta. ***B***, Summary of the selected VGAT, PV, and CB1-R puncta from ***A***. ***C***, The density of synaptic VGAT, PV and CB1-R puncta (VGAT $p = 0.19$; PV $p = 0.02$; CB1-R $p = 0.36$). ***D***, The mean intensity of synaptic puncta (VGAT $p = 0.51$; PV $p < 0.0005$; CB1-R $p = 0.02$). ***E***, The mean area of synaptic puncta (VGAT $p = 0.93$; PV $p = 0.11$; CB1-R $p = 0.05$). ***F***, Soma size of L5 pyramidal cells ($p = 0.20$; *t* test). ***F***, Correlation between L5 soma size and VGAT synaptic puncta density. Data in ***C–G*** from 49 CTL cells and 34 SPD cells (6 rats per group, 2 hemispheres). Statistical range: $^{*}p \leq 0.05$, $^{**}p < 0.01$, $^{***}p < 0.001$.

were separated from their cage mate by a Plexiglas wall, which allowed smelling, hearing, seeing and communicating, but not physical interaction and playing. After the SPD period, the wall was removed and pair-wise social housing was maintained until adulthood when experiments were performed (postnatal week 8–10). Control (CTL) rats were housed in pairs during the entire period. We performed voltage-clamp recordings from layer 5 (L5) pyramidal cells of the medial PFC (mPFC), the main output neurons, in slices prepared from adult SPD and CTL rats to assess the impact of SPD on PFC circuitry development (Fig. 1*A–C*). We found that the frequency and amplitude of spontaneous IPSCs (sIPSCs) was reduced in SPD rats (Fig. 1*D*,*E*). By contrast, spontaneous EPSCs (sEPSCs) were unaffected (Fig. 1*F*,*G*). The frequency of miniature inhibitory currents (mIPSCs) was also reduced in SPD slices (Fig. 1*H*), while mIPSC amplitudes (Fig. 1*I*) were not affected. The reduction in mIPSC frequency in SPD slices was accompanied by an increase in the average rise time (Fig. 1*J*), suggesting that particularly mIPSCs with fast kinetics were lost. Decay kinetics (Fig. 1*K*) and intrinsic excitability (Fig. 2*A–C*) were unaffected. Together, these data indicate that SPD leads to selective reduction in GABAergic synaptic inputs onto L5 pyramidal cells in the adult mPFC.

A reduction in mIPSCs with fast rise times suggests that inhibitory synapses at perisomatic locations were affected. Perisomatic synapses are made by parvalbumin (PV) and cholecystokinin (CCK) basket cells (Whissell et al., 2015), of which only the latter express the cannabinoid receptor 1 (CB1-R; Katona et al., 1999). We performed immunohistochemistry on the mPFC of adult SPD and CTL rats and quantified the number of GAD67-positive and PV-positive cell bodies (Fig. 3*A*). The density of GAD67-positive interneurons (Fig. 3*B*) and PV-positive cells (Fig. 3*C*) in the mPFC was not different between SPD and CTL rats. We then quantified inhibitory synaptic markers around the soma of L5 pyramidal neurons, using NeuN staining to draw a narrow band around the soma of individual pyramidal neurons and analyze the synaptic PV and CB1 puncta within this band (Fig. 4*A*,*B*). The density of VGAT puncta was not different in SPD and CTL tissue, but the density of PV synapses (colocalizing with VGAT) was significantly lower in SPD tissue compared with CTL tissue (Fig. 4*C*). The density of CB1-R synapses was not altered. In addition, synaptic PV and CB1-R puncta intensity was decreased in SPD tissue (Fig. 4*D*). This reduction was specific as VGAT puncta intensity was

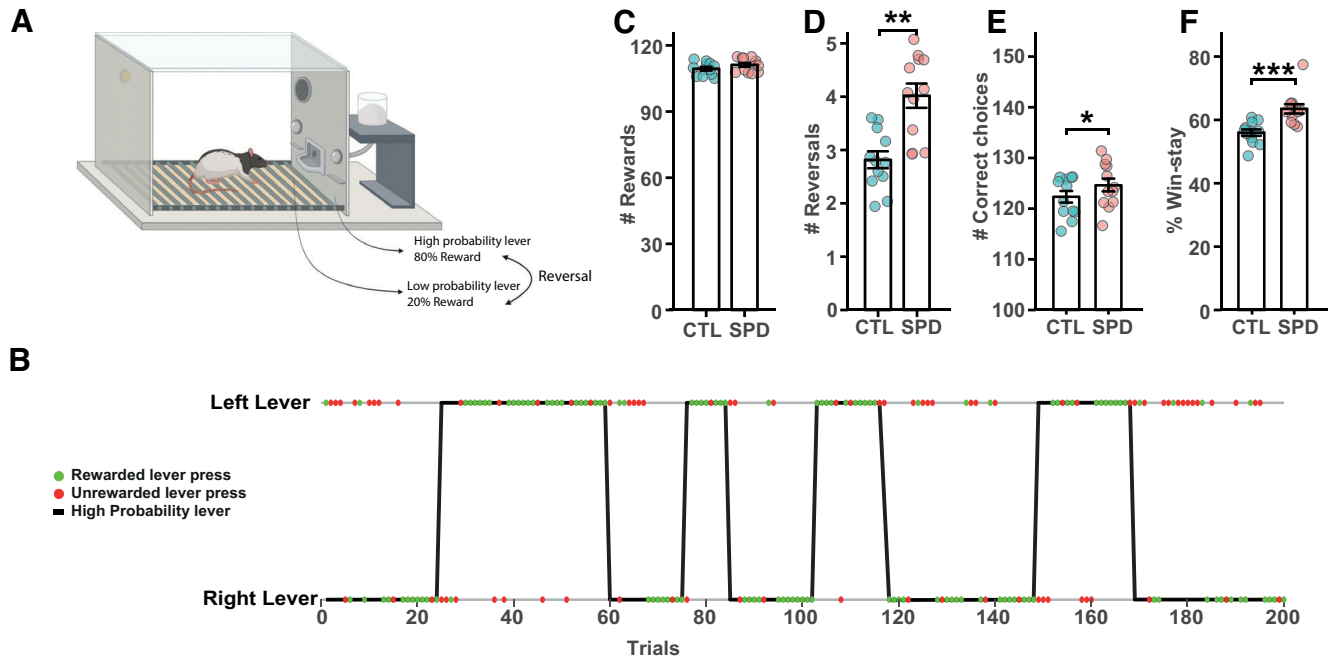

Figure 5. Altered PRL performance after SPD. ***A***, Probabilistic reversal learning task design. Reversals occur when the rat has pressed the high probability lever eight consecutive times. ***B***, Representation of the 200 lever presses of an example session. Green and red dots represent rewarded and unrewarded lever presses, respectively. A reversal is indicated by the change of the high probability lever. ***C***, Average number of rewards for CTL and SPD rats ($p = 0.16$; *t* test). ***D***, Average number of reversals ($p = 0.001$; *t* test). ***E***, Average number of correct responses ($p = 0.032$; *t* test). ***F***, Average percentage of win-stay choices ($p = 0.001$; *t* test). Data in ***C–F*** from 12 CTL and 12 SPD rats (batch 1). Statistical range: $^{*}p \leq 0.05$, $^{**}p < 0.01$, $^{***}p < 0.001$.

similar in SPD and CTL tissue (Fig. 4*D*). Puncta size was not much affected, although synaptic CB1-R puncta were slightly larger in SPD tissue (Fig. 4*E*). We verified that somata of L5 pyramidal cells had similar size in SPD and CTL tissue (Fig. 4*F*) and synaptic density was not correlated with cell size (Fig. 4*G*). Together, these data show that SPD results in a decrease in inhibitory synaptic input to L5 pyramidal cells in the adult PFC, with differential effects on perisomatic PV and CB1-R synapses.

In order to assess the impact of SPD on cognitive flexibility, a PFC-dependent probabilistic reversal learning (PRL) task was used (Fig. 5*A*,*B*; Dalton et al., 2016; Verharen et al., 2020). In this task, responding on the "correct" and "incorrect" levers was rewarded on 80% and 20% of trials, respectively, and position of the "correct" and "incorrect" levers switched after eight consecutive responses on the "correct" lever. Rats in the SPD and CTL groups readily acquired the task and achieved a comparable performance level in terms of rewards obtained (Fig. 5*C*). Remarkably, SPD rats completed more reversals (Fig. 5*D*) and made more correct choices (Fig. 5*E*) compared with CTL rats. SPD rats showed an enhanced tendency to stay at a lever after it was rewarded (so-called "win-stay" behavior; Fig. 5*F*). These observations indicate that cognitive performance in adult rats was altered after SPD.

Early behavioral studies have shown that behavioral performance after social isolation can be partially rescued by allowing the rats daily play for a short amount of time (Einon et al., 1978; Potegal and Einon, 1989). The idea behind these studies was that a daily limited, but condensed play time should be sufficient to prevent neural and behavioral changes. We therefore introduced a second group of SPD rats that was allowed to play daily for 1 h with their cage mate during the deprivation period (SPD1h). We quantified pinning and pouncing, the most characteristic social play behaviors in rats (Panksepp and Beatty, 1980; Vanderschuren et al., 1995b), as well as social and nonsocial exploration during the play sessions of the SPD1h rats (Fig. 6*A–D*). SPD1h rats made ~200 pins and ~300 pounces per hour, which was comparable to rats in other studies that were isolated for 24 h (Niesink and Van Ree, 1989; Vanderschuren et al., 1995a, b, 2008; Achterberg et al., 2016). This is four to six times higher compared with socially housed rats of the same age, which typically show 40–60 pins per hour (Vanderschuren et al., 2008; Schneider et al., 2016b). Quantification of the social interactions showed that around 75% of pins and pounces occurred in the first half hour of the session (Fig. 6*E–F*). This indicates that SPD1h rats experienced a substantial amount of the daily social play that control rats are normally experiencing (equivalent to 4–6 h, ~50% of daily play time), but in a very condensed time.

We then repeated the PRL task with three groups of rats: control, SPD, and SPD1h. Rats of all three groups learned the task equally well and gained similar numbers of rewards (Fig. 7*A*). To examine possible differences between the groups, we analyzed the number of reversals per session (Fig. 7*B*). Consistent with our earlier results (Fig. 5*D*), SPD rats tended to complete more reversals per session than CTL rats (Fig. 7*B*), but this difference did not reach statistical significance. This was probably because of a ceiling effect because of the higher overall performance of all rats compared with the previous PRL experiment (see Materials and Methods and compare values in Figs. 7*B* and 5*D*). However, when we normalized and pooled the data from both batches, the number of reversals in the SPD group was clearly above CTL ($p < 0.001$; two-way ANOVA with Tukey's *post hoc* test). In addition, we observed that SPD rats made more correct choices compared with CTL rats (Fig. 7*C*), establishing an important independent confirmation of our earlier results (Fig. 5*E*).

At first glance, the 1-h daily play sessions did not seem to affect PRL performance in SPD rats, as SPD1h rats made more correct choices compared with CTL rats (Fig. 7*C*), echoing the behavior of SPD rats during the sessions. However, the performance in reversal completion appeared qualitatively different as

the SPD1h rats resembled the SPD group during the initial sessions, but performed closer to the control group in later sessions (Fig. 7*B*). To further explore possible differences between the groups in more detail, we assessed win-stay behavior over the course of the sessions. Consistent with Figure 5*F*, we observed consistently more win-stay choices in the SPD group compared with CTL rats in all sessions, but this effect was not present in the SPD1h group (Fig. 7*D*). This difference between SPD and SPD1h group was even clearer when we pooled the data from both batches (Fig. 7*E*,*F*). When we normalized the win-stay responses in each group to the CTL group, SPD choices are clearly different from both other groups. The SPD1h curve resembled the SPD curve in some of the earlier sessions, but then remained closer to the CTL curve toward the later sessions. There was no difference between groups in their choices after nonrewarded trials (CTL: 45 ± 8% SPD: 45 ± 7%; SPD1h: 45 ± 7%; ANOVA $p = 0.86$).

We next performed computational modeling analysis of the behavioral data (Verharen et al., 2018, 2020) to reveal possible alterations in the component processes subserving probabilistic reversal learning. This model-based approach investigates task performance based on an extended history of trial outcomes, and not merely the most recent outcome, such as win-stay and lose-stay measures do, providing a more in-depth analysis of the task strategy used by the animals. We compared different computational models to describe the behavioral choices of the rats. The simplest random model assumes that animals always randomly choose a lever to press. A family of three heuristic models assumes simple practical strategies to complete the task (e.g., win-stay, lose-shift, etc.). Finally, the four Q learning models integrate sensitivity to positive and negative feedback, and weigh exploration versus exploitation (for details, see Materials and Methods). We calculated Akaike information criterion (AIC) scores to assess how well the behavioral choices were described by the different computational models (Fig. 8*A*). Although in all groups Q learning models (models 5–8) were generally better than the heuristic win-stay models (models 2 and 3) to describe behavioral choices, models that contained a "stickiness" parameter (models 4 and 7) always performed best (Fig. 8*A*). The behavior of CTL rats was best described by a Q-learning model in all sessions (Fig. 8*B*, left panel), but the SPD and SPD1h rats shifted toward behavior congruent with a simpler heuristic strategy as reversal learning progressed (Fig. 8*B*, middle and right panel), showing a tendency to remain at the previously chosen lever. Thus, SPD rats, with or without daily playtimes, switched from a learning-based strategy to a more perseverative strategy, whereas CTL rats continued learning throughout training. These data indicate that juvenile SPD alters PFC function and cognitive flexibility in adulthood. Furthermore, it shows that 1 h daily play during SPD only partially restores the cognitive performance in SPD rats.

To check whether the partial rescue in PRL behavior of the SPD1h rats was because of a rescue of the inhibitory microcircuitry in the mPFC, we recorded miniature inhibitory currents (mIPSCs) in prefrontal slices from all three groups. Consistent with our earlier results (Fig. 1*H*), a clear reduction in mIPSC frequency was found in the SPD group compared with CTL rats (Fig. 9*B*). This reduction was similar in the SPD and SPD1h slices, indicating that daily playtimes during the play deprivation period did not affect the development of PFC inhibition (Fig. 9*B*). Amplitudes of the events were not different between groups (Fig. 9*C*).

Our findings demonstrate that the organization of the adult GABAergic system in the mPFC of rats is robustly altered when rats are deprived of social play behavior during development, with important consequences for cognitive flexibility. The inclusion of daily play sessions during the SPD period failed to rescue the reduction in PFC GABAergic synapses and only partially restored the cognitive performance in a PFC-dependent PRL task.

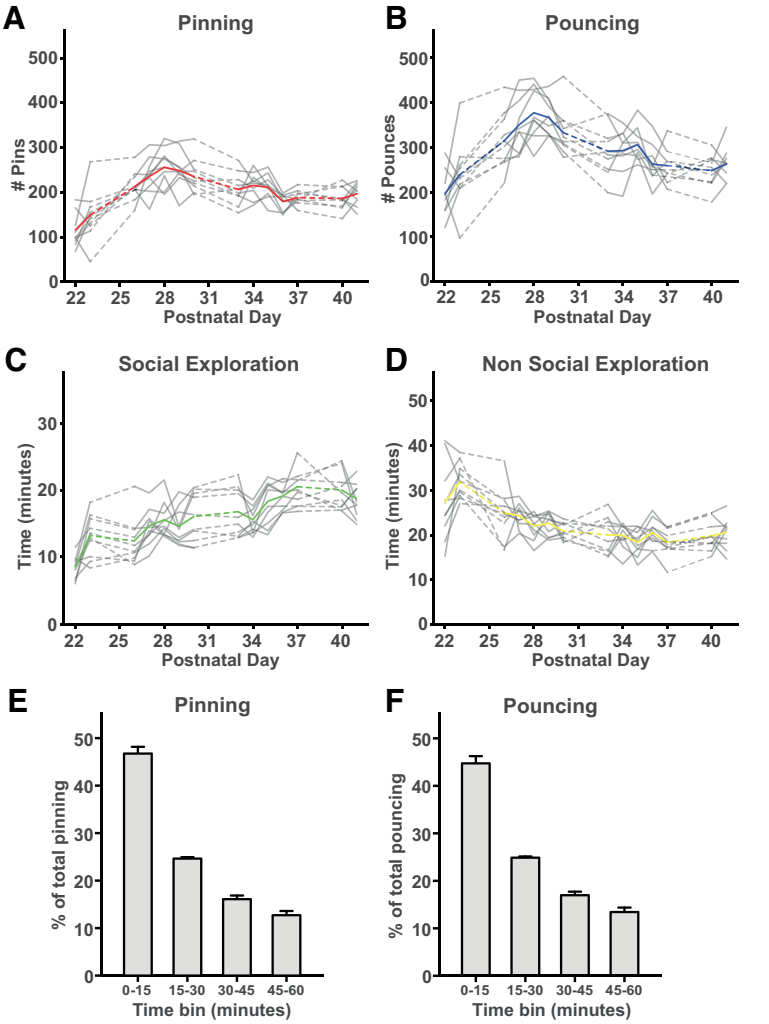

Figure 6. Social behavior during 1-h play sessions. ***A***, ***B***, The frequency of (***A***) pinning and (***B***) pouncing of the SPD1h rats during the 1-h play sessions per day. ***C***, ***D***, The time spent in (***C***) social and (***D***) nonsocial exploration. Each gray line represents a pair of rats with the colored line representing the groups' average. ***E***, ***F***, The behavioral readouts of social play are expressed as fraction of the total. For both (***E***) pinning and (***F***) pouncing, the amount was separated in bins of 15 min. Data from 10 pairs of SPD1h rats.

Discussion

Like most other mammalian species, young rats display an abundance of a particular, highly rewarding and energetic form of social behavior, termed social play behavior (Panksepp et al.,

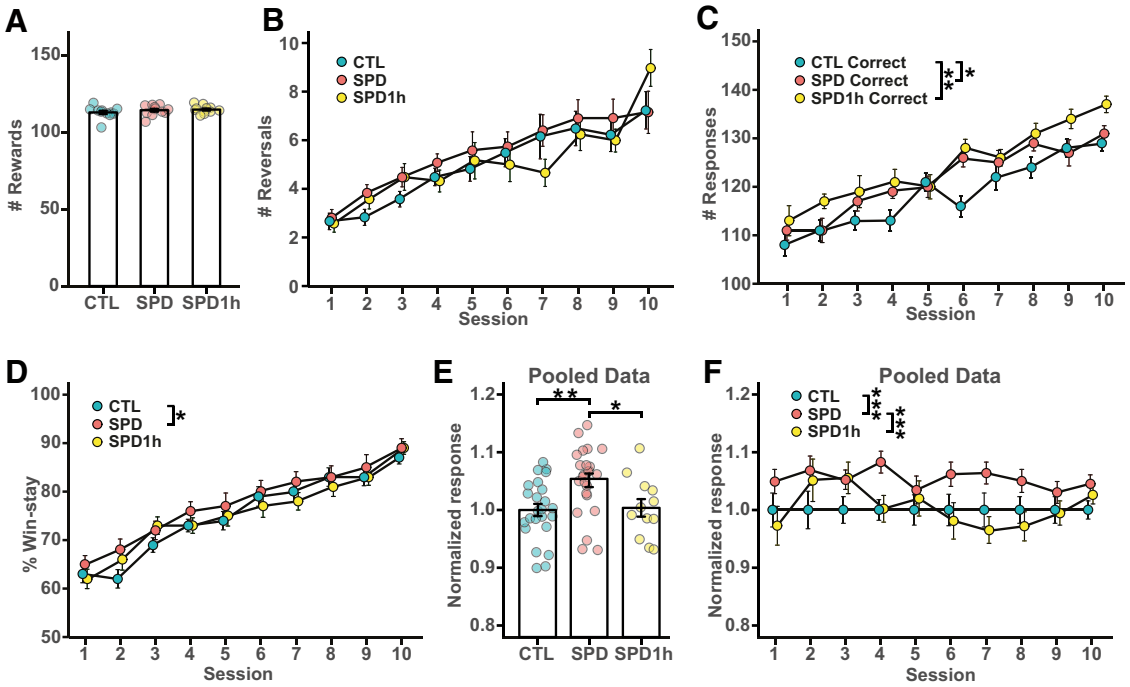

Figure 7. Behavioral analysis of altered PRL performance after SPD. ***A***, Number of sucrose rewards for CTL, SPD, and SPD1h rats ($p = 0.33$ ANOVA). ***B***, Number of reversals per session ($p = 0.22$ ANOVA). ***C***, Number of correct lever presses per session ($p < 0.001$ ANOVA; CTL-SPD, $p = 0.050$; CTL-SPD1h, $p = 0.006$; SPD-SPD1h, $p = 0.72$). ***D***, Normalized win-stay responses per session ($p < 0.001$ ANOVA; CTL-SPD, $p = 0.04$; CTL-SPD1h, $p = 0.97$; SPD-SPD1h, $p = 0.07$). ***E***, Normalized average win-stay responses (pooled data from both batches; $p < 0.001$ ANOVA; CTL-SPD, $p = 0.003$; CTL-SPD1h, $p = 0.97$; SPD-SPD1h, $p = 0.03$). ***F***, Normalized average win-stay responses per session ($p < 0.001$, two-way ANOVA; CTL-SPD, $p < 0.001$; CTL-SPD1h, $p = 0.74$; SPD-SPD1h, $p < 0.001$). Data in ***A–D*** from 12 CTL, 12 SPD and 12 SPD1h rats (batch 2); data in ***E***, ***F*** from 24 CTL, 24 SPD and 12 SPD1h rats (batches 1 and 2 pooled). Statistical range: $^*p \leq 0.05$, $^{**}p < 0.01$, $^{***}p < 0.001$.

1984; Vanderschuren et al., 1997; Pellis and Pellis, 2009; Achterberg et al., 2016). Playing with peers is thought to allow young animals to experiment with their behavioral repertoire, and to provide practice scenarios to obtain the social, cognitive and emotional skills to become capable adults who can easily navigate a changeable world (Spinka et al., 2001; Pellis and Pellis, 2009; Vanderschuren and Trezza, 2014; Larsen and Luna, 2018). Here, we found that social play deprivation from P21 until P42 reduces specific inhibitory connections in the PFC and affects cognitive skills in adulthood. Importantly, after the temporary deprivation when rats were young, the animals had ample opportunity for social interaction during the weeks before testing. However, even after several weeks of unrestricted social interactions, pronounced changes in PFC function and cognition were present. This emphasizes the importance of early postweaning social play, consistent with earlier studies that identified this time window as a critical period for PFC maturation and behavioral development (Einon and Morgan, 1977; Hol et al., 1999; van den Berg et al., 1999; Lukkes et al., 2009; Kolb et al., 2012; Whitaker et al., 2013). Furthermore, previous studies have suggested that a daily limited, but condensed play time should be sufficient to prevent the neural and behavioral changes observed (Einon and Morgan, 1977; Potegal and Einon, 1989). However, we found that although 1 h of daily condensed play (roughly equivalent to 4–6 h of "normal" play) partially rescued cognitive performance in SPD rats, the reduction in PFC inhibition remained unaltered. Our data therefore suggest that the experience of unrestricted juvenile social play is crucial to instruct the development of specific inhibitory connections in the PFC and to shape adaptive cognitive strategies in the adult brain.

Social play enhances neuronal activity in a broad network of limbic and corticostriatal structures (Gordon et al., 2002, 2003; van Kerkhof et al., 2013b). This integrated neuronal activity likely drives PFC maturation during development, analogous to the well-described experience-dependent maturation of cortical sensory circuits, which requires appropriate sensory activation during development (Hensch, 2005; Gainey and Feldman, 2017). To our knowledge, our study is the first to report a specific and robust synaptic alteration in the adult PFC after SPD. We observed that perisomatic inhibition onto L5 cells was reduced in the adult mPFC after SPD. We found a ~30% reduction in mIPSC frequency, associated with a comparable reduction in perisomatic PV synapses, in line with previous observations in sensory cortex showing a reduction in inhibition after sensory deprivation (Hensch et al., 1998; Morales et al., 2002; Chattopadhyaya et al., 2004; Jiao et al., 2006; Mowery et al., 2019; Reh et al., 2020). In addition, we report a reduced level of PV and CB1 expression in prefrontal L5 inhibitory synapses after SPD. This may indicate a reduced activity level in PV cells (Donato et al., 2013; Caballero et al., 2014) and an altered endocannabinoid tone (Sciolino et al., 2010; Schneider et al., 2016a).

Alterations in PV cells during development are shown to shape cognitive capacities in adulthood (Donato et al., 2015; Mukherjee et al., 2019; Canetta et al., 2022). Changes in PFC network activity directly affect cognitive and social skills (Yizhar et al., 2011; Dalton et al., 2016; Verharen et al., 2020), but it is hard to pinpoint how reduced PV innervation of L5 cells will affect PFC function. A reduction in PFC inhibition has previously been linked to impaired cognitive flexibility (Gruber et al., 2010), and a direct link between PFC PV cell activity and social behavior was recently demonstrated (Bicks et al., 2020; Sun et al., 2020). From our data it is not clear whether the reduction in inhibitory drive to L5 cells will lead to enhanced activity in downstream brain regions or whether it actually compensates for a change in

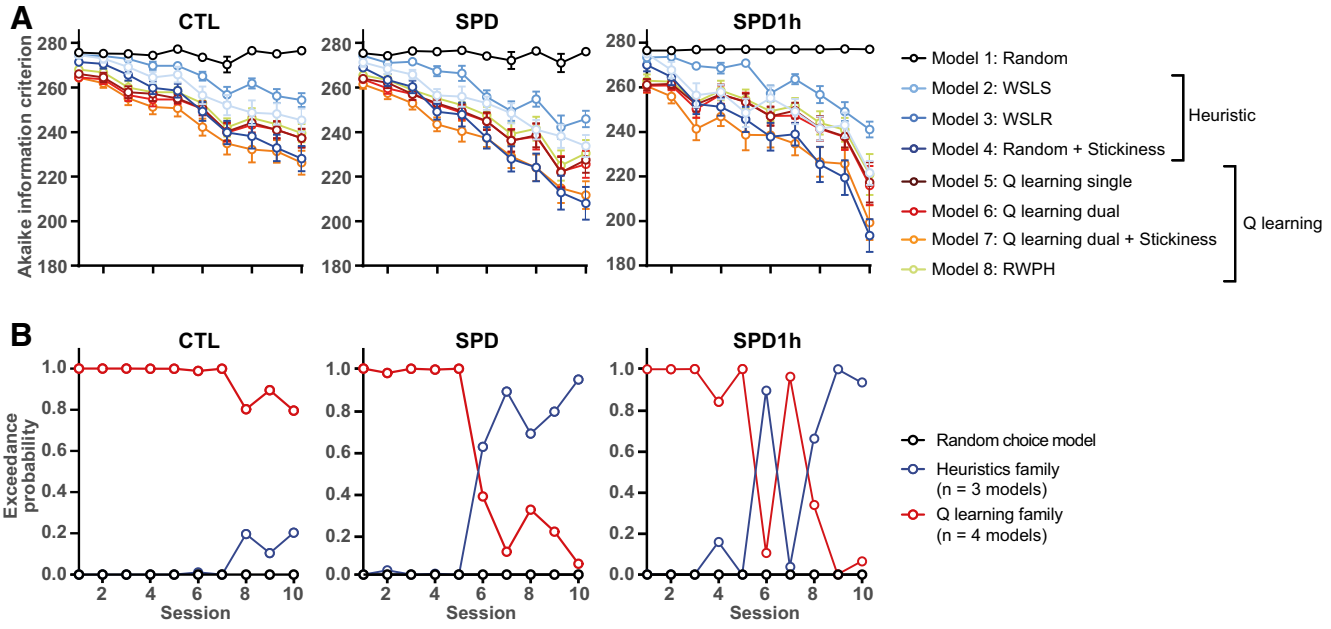

Figure 8. Trial-by-trial analysis of PRL performance. ***A***, Akaike information criterion (AIC) scores for the seven models. Please note that lower AIC scores reflect a better fit between model predictions and behavioral data. ***B***, Exceedance probability for different families of computational models (Random choice, Heuristics, and Q-learning families) based on Bayesian model selection for the three groups (CTL, SPD, and SPD1h rats).

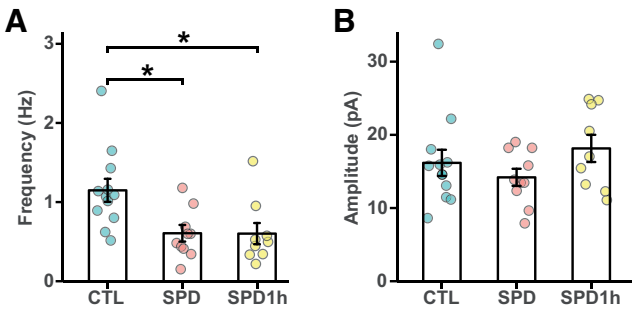

Figure 9. Reduced prefrontal inhibition in L5 pyramidal cells in SPD and SPD1h slices. ***A***, Frequency of mIPSCs in CTL, SPD, and SPD1h slices (ANOVA $p = 0.0049$, Tukey's test: CTL vs SPD $p = 0.011$; CTL vs SPD1h $p = 0.017$; SPD vs SPD1h $p = 0.99$). ***B***, Amplitude of mIPSCs in CTL, SPD, and SPD1h slices (ANOVA $p = 0.29$). Data from 12 CTL, 10 SPD, and 9 SPD1h cells (6 rats per group). Statistical range: $^*p \leq 0.05$.

upstream activity or connectivity within the local mPFC network. Interestingly, recent studies showed that prefrontal PV and CCK cells, which provide the perisomatic inhibition on L5 cells, receive specific input from the ventral hippocampus (Liu et al., 2020), while the thalamic drive appears less important for PV cells in the PFC (Benoit et al., 2022). It will be important to further explore other synaptic changes in the intricate PFC circuitry after SPD and their consequences for PFC-driven modulation of behavior.

In this study, we observed that adult rats which had experienced SPD displayed a different behavioral strategy in the PRL task compared with CTL animals. PRL performance depends on complex interactions between several component processes, including the sensitivity to positive and negative feedback, response persistence and exploration versus exploitation, each of which requires functional activity in distinct PFC regions (Verharen et al., 2018, 2020), as well as brain regions outside the PFC (Izquierdo et al., 2017). CTL rats seemed to follow a sophisticated cognitive strategy which was well-described by a Q-learning model. Our data indicate that SPD rats made more correct choices by using a simplified strategy, in which they relied less on feedback-driven learning, and more on perseverance (represented by a "stickiness" parameter in our models). This is probably cognitively less demanding (Christie and Schrater, 2015), and may therefore be preferred under certain conditions, especially if this does not lead to a reduction in reward. A similar increase in reversals was also reported after prelimbic mPFC inactivation (Dalton et al., 2016), suggesting that the mPFC may be less involved in PRL performance in SPD rats compared with CTL rats.

Our data demonstrate that social play behavior is of critical importance for the development of PFC circuitry and function, and PFC-dependent cognitive processes. At this point, we can only speculate whether it is the social, cognitive, emotional, sensory or physical aspects of social play, or their interaction, that determines proper PFC development. We observed that 1 h of daily playtime during the deprivation period could not rescue the reduction in prefrontal IPSCs, but it partially rescued behavior in adulthood. Play is not displayed continuously by young rats, but appears in peaks of relatively short duration across the day (Melotti et al., 2014; Lampe et al., 2019). We observed that SPD1h rats played very intensely during the first 15–30 min of each play session resulting in a total amount of play that makes up a substantial fraction of the daily play that socially housed CTL rats show at this age. As this was not enough to prevent the reduction in prefrontal inhibition after SPD, it suggests the necessity of unrestricted, voluntarily elicited or repeated play for proper PFC maturation. Our observation that the behavior of SPD1hr fell in between SPD and CTL rats, while their reduction in mPFC inhibition was similar to SPD rats, suggests that the partial rescue of behavior involves compensatory changes other than L5 inhibition, and further studies will be needed to elucidate these. Together, our results demonstrate a key role for juvenile social play in the development of perisomatic inhibition in the PFC and PFC-dependent cognitive flexibility.

References

Achterberg EJM, Van Kerkhof LWM, Servadio M, Van Swieten MMH, Houwing DJ, Aalderink M, Driel NV, Trezza V, Vanderschuren LJMJ (2016) Contrasting roles of dopamine and noradrenaline in the motivational properties of social play behavior in rats. Neuropsychopharmacology 41:858–868.

Baarendse PJJ, Counotte DS, O'Donnell P, Vanderschuren LJMJ (2013) Early social experience is critical for the development of cognitive control and dopamine modulation of prefrontal cortex function. Neuropsychopharmacology 38:1485–1494.

Baenninger LP (1967) Comparison of behavioural development in socially isolated and grouped rats. Anim Behav 15:312–323.

Bari A, Theobald DE, Caprioli D, Mar AC, Aidoo-Micah A, Dalley JW, Robbins TW (2010) Serotonin modulates sensitivity to reward and negative feedback in a probabilistic reversal learning task in rats. Neuropsychopharmacol 35:1290–1301.

Bell HC, McCaffrey DR, Forgie ML, Kolb B, Pellis SM (2009) The role of the medial prefrontal cortex in the play fighting of rats. Behav Neurosci 123:1158–1168.

Bell HC, Pellis SM, Kolb B (2010) Juvenile peer play experience and the development of the orbitofrontal and medial prefrontal cortices. Behav Brain Res 207:7–13.

Benoit LJ, Holt ES, Posani L, Fusi S, Harris AZ, Canetta S, Kellendonk C (2022) Adolescent thalamic inhibition leads to long-lasting impairments in prefrontal cortex function. Nat Neurosci 25:714–725.

Bicks LK, Yamamuro K, Flanigan ME, Kim JM, Kato D, Lucas EK, Koike H, Peng MS, Brady DM, Chandrasekaran S, Norman KJ, Smith MR, Clem RL, Russo SJ, Akbarian S, Morishita H (2020) Prefrontal parvalbumin interneurons require juvenile social experience to establish adult social behavior. Nat Commun 11:1003.

Caballero A, Flores-Barrera E, Cass DK, Tseng KY (2014) Differential regulation of parvalbumin and calretinin interneurons in the prefrontal cortex during adolescence. Brain Struct Funct 219:395–406.

Canetta SE, Holt ES, Benoit LJ, Teboul E, Sahyoun GM, Ogden RT, Harris AZ, Kellendonk C (2022) Mature parvalbumin interneuron function in prefrontal cortex requires activity during a postnatal sensitive period. bioRxiv 433943.

Chattopadhyaya B, Cristo GD, Higashiyama H, Knott GW, Kuhlman SJ, Welker E, Huang ZJ, Di Cristo G (2004) Experience and activity-dependent maturation of perisomatic GABAergic innervation in primary visual cortex during a postnatal critical period. J Neurosci 24:9598–9611.

Christie ST, Schrater P (2015) Cognitive cost as dynamic allocation of energetic resources. Front Neurosci 9:1–15.

Dalton GL, Wang NY, Phillips AG, Floresco SB (2016) Multifaceted contributions by different regions of the orbitofrontal and medial prefrontal cortex to probabilistic reversal learning. J Neurosci 36:1996–2006.

Donato F, Rompani SB, Caroni P (2013) Parvalbumin-expressing basket-cell network plasticity induced by experience regulates adult learning. Nature 504:272–276.

Donato F, Chowdhury A, Lahr M, Caroni P (2015) Early- and late-born parvalbumin basket cell subpopulations exhibiting distinct regulation and roles in learning. Neuron 85:770–786.

Douglas RJ, Martin KAC (2004) Neuronal circuits of the neocortex. Annu Rev Neurosci 27:419–451.

Einon DF, Morgan MJ (1977) Critical period for social isolation. Dev Psychobiol 10:123–132.

Einon DF, Morgan MJ, Kibbler CC (1978) Brief periods of socialization and later behavior in the rat. Dev Psychobiol 11:213–225.

Floresco SB, Block AE, Tse MTL (2008) Inactivation of the medial prefrontal cortex of the rat impairs strategy set-shifting, but not reversal learning, using a novel, automated procedure. Behav Brain Res 190:85–96.

Frith CD, Frith U (2012) Mechanisms of social cognition. Annu Rev Psychol 63:287–313.

Gainey MA, Feldman DE (2017) Multiple shared mechanisms for homeostatic plasticity in rodent somatosensory and visual cortex. Phil Trans R Soc B 372:20160157.

Gordon NS, Kollack-Walker S, Akil H, Panksepp J (2002) Expression of c-fos gene activation during rough and tumble play in juvenile rats. Brain Res Bull 57:651–659.

Gordon NS, Burke S, Akil H, Watson SJ, Panksepp J (2003) Socially-induced brain 'fertilization': play promotes brain derived neurotrophic factor transcription in the amygdala and dorsolateral frontal cortex in juvenile rats. Neurosci Lett 341:17–20.

Gruber AJ, Calhoon GG, Shusterman I, Schoenbaum G, Roesch MR, O'Donnell P (2010) More is less: a disinhibited prefrontal cortex impairs cognitive flexibility. J Neurosci 30:17102–17110.

Hensch TK (2005) Critical period plasticity in local cortical circuits. Nat Rev Neurosci 6:877–888.

Hensch T, Fagiolini M, Mataga N, Stryker M, Baekkeskov S, Kash S (1998) Local GABA circuit control of experience-dependent plasticity in developing visual cortex. Science 282:1504–1508.

Hol T, Van den Berg CL, Van Ree JM, Spruijt BM (1999) Isolation during the play period in infancy decreases adult social interactions in rats. Behav Brain Res 100:91–97.

Izquierdo A, Brigman JL, Radke AK, Rudebeck PH, Holmes A (2017) The neural basis of reversal learning: an updated perspective. Neuroscience 345:12–26.

Jiao Y, Zhang C, Yanagawa Y, Sun QQ (2006) Major effects of sensory experiences on the neocortical inhibitory circuits. J Neurosci 26:8691–8701.

Katona I, Sperlágh B, Sík A, Käfalvi A, Vizi ES, Mackie K, Freund TF (1999) Presynaptically located CB1 cannabinoid receptors regulate GABA release from axon terminals of specific hippocampal interneurons. J Neurosci 19:4544–4558.

Kolb B, Mychasiuk R, Muhammad A, Li Y, Frost DO, Gibb R (2012) Experience and the developing prefrontal cortex. Proc Natl Acad Sci U S A 109:17186–17193.

Lampe JF, Ruchti S, Burman O, Würbel H, Melotti L (2019) Play like me: similarity in playfulness promotes social play. PLoS One 14:e0224282.

Larsen B, Luna B (2018) Adolescence as a neurobiological critical period for the development of higher-order cognition. Neurosci Biobehav Rev 94:179–195.

Leussis MP, Lawson K, Stone K, Andersen SL (2008) The enduring effects of an adolescent social stressor on synaptic density, part II: poststress reversal of synaptic loss in the cortex by adinazolam and MK-801. Synapse 62:185–192.

Liu X, Dimidschstein J, Fishell G, Carter AG (2020) Hippocampal inputs engage cck+ interneurons to mediate endocannabinoid-modulated feedforward inhibition in the prefrontal cortex. Elife 9:e55267.

Lukkes JL, Watt MJ, Lowry CA, Forster GL (2009) Consequences of post-weaning social isolation on anxiety behavior and related neural circuits in rodents. Front Behav Neurosci 3:18.

Meaney MJ, Stewart J (1981) A descriptive study of social development in the rat (*Rattus norvegicus*). Anim Behav 29:34–45.

Melotti L, Bailoo J, Murphy E, Burman O, Wurbel H (2014) Play in rats: association across contexts and types, and analysis of structure. Anim Behav Cogn 1:489–501.

Miller EK, Cohen JD (2001) An integrative theory of prefrontal cortex function. Annu Rev Neurosci 24:167–202.

Morales B, Choi SY, Kirkwood A (2002) Dark rearing alters the development of GABAergic transmission in visual cortex. J Neurosci 22:8084–8090.

Mowery TM, Caras ML, Hassan SI, Wang DJ, Dimidschstein J, Fishell G, Sanes DH (2019) Preserving inhibition during developmental hearing loss rescues auditory learning and perception. J Neurosci 39:8347–8361.

Mukherjee A, Carvalho F, Eliez S, Caroni P (2019) Long-lasting rescue of network and cognitive dysfunction in a genetic schizophrenia model. Cell 178:1387–1402.e14.

Niesink RJM, Van Ree JM (1989) Involvement of opioid and dopaminergic systems in isolation-induced pinning and social grooming of young rats. Neuropharmacology 28:411–418.

Panksepp J (1981) The ontogeny of play in rats. Dev Psychobiol 14:327–332.

Panksepp J, Beatty WW (1980) Social deprivation and play in rats. Behav Neural Biol 30:197–206.

Panksepp J, Siviy S, Normansell L (1984) The psychobiology of play: theoretical and methodological perspectives. Neurosci Biobehav Rev 8:465–492.

Paxinos G, Watson C (2007) The rat brain in stereotaxic coordinates, Ed 6. San Diego: Academic Press Inc.

Pellis SM, Pellis V (2009) The playful brain: venturing to the limits of neuroscience. London: Oneworld Publications.

Penny WD, Stephan KE, Daunizeau J, Rosa MJ, Friston KJ, Schofield TM, Leff AP (2010) Comparing families of dynamic causal models. PLoS Comput Biol 6:e1000709.

Potegal M, Einon D (1989) Aggressive behaviors in adult rats deprived of playfighting experience as juveniles. Dev Psychobiol 22:159–172.

Reh RK, Dias BG, Nelson IIC, Kaufer D, Werker JF, Kolb B, Levine JD, Hensch TK (2020) Critical period regulation across multiple timescales. Proc Natl Acad Sci U S A 117:23242–23251.

Rescorla RA, Wagner AR (1972) A theory of Pavlovian conditioning: variations in the effectiveness of reinforcement and nonreinforcement. In: Classical conditioning II (Black AH, Prokasy WF, eds). New York: Appleton-Century-Crofts.

Rigoux L, Stephan KE, Friston KJ, Daunizeau J (2014) Bayesian model selection for group studies - revisited. Neuroimage 84:971–985.

Rilling J, Sanfey A (2011) The neuroscience of social decision-making. Annu Rev Psychol 62:23–48.

Rupert DD, Shea SD (2022) Parvalbumin-positive interneurons regulate cortical sensory plasticity in adulthood and development through shared mechanisms. Front Neural Circuits 16:1–12.

Schneider P, Bindila L, Schmahl C, Bohus M, Meyer-Lindenberg A, Lutz B, Spanagel R, Schneider M (2016a) Adverse social experiences in adolescent rats result in enduring effects on social competence, pain sensitivity and endocannabinoid signaling. Front Behav Neurosci 10:1–16.

Schneider P, Pätz M, Spanagel R, Schneider M (2016b) Adolescent social rejection alters pain processing in a CB1 receptor dependent manner. Eur Neuropsychopharmacol 26:1201–1212.

Sciolino NR, Bortolato M, Eisenstein SA, Fu J, Oveisi F, Hohmann AG, Piomelli D (2010) Social isolation and chronic handling alter endocannabinoid signaling and behavioral reactivity to context in adult rats. Neuroscience 168:371–386.

Spinka M, Newberry RC, Bekoff M (2001) Mammalian play: training for the unexpected. Q Rev Biol 76:141–168.

Sun Q, Li X, Li A, Zhang J, Ding Z, Gong H, Luo Q (2020) Ventral hippocampal-prefrontal interaction affects social behavior via parvalbumin positive neurons in the medial prefrontal cortex. iScience 23:100894.

Turrigiano GG, Nelson SB (2004) Homeostatic plasticity in the developing nervous system. Nat Rev Neurosci 5:97–107.

van den Berg CL, Hol T, Van Ree JM, Spruijt BM, Everts H, Koolhaas JM (1999) Play is indispensable for an adequate development of coping with social challenges in the rat. Dev Psychobiol 34:129–138.

van Kerkhof LW, Damsteegt R, Trezza V, Voorn P, Vanderschuren LJ (2013a) Social play behavior in adolescent rats is mediated by functional activity in medial prefrontal cortex and striatum. Neuropsychopharmacology 38:1899–1909.

van Kerkhof LWM, Trezza V, Mulder T, Gao P, Voorn P, Vanderschuren LJMJ (2013b) Cellular activation in limbic brain systems during social play behaviour in rats. Brain Struct Funct 219:1181–1211.

Vanderschuren LJMJ, Trezza V (2014) What the laboratory rat has taught us about social play behavior: role in behavioral development and neural mechanisms. Curr Top Behav Neurosci 16:189–212.

Vanderschuren LJMJ, Spruijt BM, Hol T, Niesink RJM, Ree JV (1995a) Sequential analysis of social play behavior in juvenile rats: effects of morphine. Behav Brain Res 72:89–95.

Vanderschuren LJMJ, Spruijt BM, Van Ree JM, Niesink RJM (1995b) Effects of morphine on different aspects of social play in juvenile rats. Psychopharmacology (Berl) 117:225–231.

Vanderschuren LJ, Niesink RJ, Van Ree JM (1997) The neurobiology of social play behavior in rats. Neurosci Biobehav Rev 21:309–326.

Vanderschuren LJMJ, Trezza V, Griffioen-Roose S, Schiepers OJG, Van Leeuwen N, De Vries TJ, Schoffelmeer ANM (2008) Methylphenidate disrupts social play behavior in adolescent rats. Neuropsychopharmacology 33:2946–2956.

Verharen JPH, De Jong JW, Roelofs TJM, Huffels CFM, Van Zessen R, Luijendijk MCM, Hamelink R, Willuhn I, Den Ouden HEM, Van Der Plasse G, Adan RAH, Vanderschuren LJMJ (2018) A neuronal mechanism underlying decision-making deficits during hyperdopaminergic states. Nat Commun 9:15.

Verharen JPH, den Ouden HEM, Adan RAH, Vanderschuren LJMJ (2020) Modulation of value-based decision making behavior by subregions of the rat prefrontal cortex. Psychopharmacology (Berl) 237:1267–1280.

Whissell PD, Cajanding JD, Fogel N, Kim JC (2015) Comparative density of CCK- and PV-GABA cells within the cortex and hippocampus. Front Neuroanat 9:1–16.

Whitaker LR, Degoulet M, Morikawa H (2013) Social deprivation enhances VTA synaptic plasticity and drug-induced contextual learning. Neuron 77:335–345.

Yizhar O, Fenno LE, Prigge M, Schneider F, Davidson TJ, O'Shea DJ, Sohal VS, Goshen I, Finkelstein J, Paz JT, Stehfest K, Fudim R, Ramakrishnan C, Huguenard JR, Hegemann P, Deisseroth K (2011) Neocortical excitation/inhibition balance in information processing and social dysfunction. Nature 477:171–178.